

Laser-plasma electron-density measurement using x-ray interferometry

Xiquan Fu and Hong Guo*

Laboratory of Light Transmission Optics, South China Normal University, Guangzhou 510631, People's Republic of China
(Received 15 February 2002; revised manuscript received 8 March 2002; published 17 June 2002)

In this paper, the propagation of x-rays in laser-produced plasma is studied both analytically and numerically. The coupling relation between phase and amplitude of x-rays is derived, the solutions with higher-order corrections are given where the higher-order electron-density gradients have been taken into account. An important parameter η was introduced, which is related to the errors of the electron-density measurement using x-ray interferometry. It is justified that so long as $\eta < 1$, the x-ray interferometry can be used for the measurement of electron density and for greater value of η , higher-order modifications are needed.

DOI: 10.1103/PhysRevE.65.067401

PACS number(s): 52.70.La, 41.20.Jb, 52.70.-m, 95.75.Kk

The characterization of the electron-density profile produced when an intense laser beam impinges on the surface of a solid material is of fundamental interest in fields such as inertial confinement fusion, x-ray lasers, and high-intensity laser-matter interactions. The plasma electron-density profile affects not only the radiation field, but also laser energy deposition and hot electron production from parametric instabilities such as stimulated Raman scattering, stimulated Brillouin scattering, and filamentation [1–3]. Hence the measurement of the laser-plasma electron density plays an important role in the diagnostics of laser-produced plasma, and the method of the refractive index of the plasma medium [2,4–9] is one of the ways used extensively. To effectively probe this high-density region of the profile, the probe wavelength must be sufficiently short so as to minimize refractive effects [2,3,10]. Early works used visible or uv light as a probe, but more recently the soft-x-ray source came to be popular since its short wavelength leads to higher critical density of the plasma, smaller diffraction effect, higher resolution, and reduction of high absorption near the critical surface [5–9,11,12]. Furthermore, the narrow-bandwidth multilayer optics can be used so that the detector can avoid being swamped by the spontaneous emission of plasma [8,9]. Conventionally, the measurement of laser-plasma electron density using x-ray interferometry is based on the relation of phase difference, $\Delta\varphi$ can be derived under WKBJ approximation [2,3], where the electron-density gradient is ignored.

In our previous work [13], a modified relation between $\Delta\varphi$ and n_e was derived and the effect of $\nabla_{\perp} n_e$ was considered to reduce the errors. However, there are still several problems left to be explored. First, the effect of the amplitude of the x-ray probe on the measurement and the relation between phase and amplitude of the x-rays propagating in plasma was not studied quantitatively; second, the region of $n_e/n_c \ll 1$ was not exactly identified and as a matter of fact, when the value of n_e/n_c increases whether x-ray interferometry and our modified relation is also valid to measure the electron density is still unclear; and lastly, whether a higher-order modification relation between $\Delta\varphi$ and n_e is needed for more precise measurement is still left to be answered. In this

paper, we intend to study the propagation of x-rays in plasma and try to derive modified solutions of phase and amplitude with higher precisions. Also, we will introduce a parameter η to reexamine the validity scope of x-ray interferometry used to measure the laser-plasma electron density.

The propagation equation for a linearly polarized x-ray probe in laser plasma can be derived from Maxwell's equations. In this paper, a one-dimensional transversal case for the sake of simplicity [13] was considered,

$$\frac{\partial^2 \psi}{\partial x^2} + 2ik \frac{\partial \psi}{\partial z} - \frac{n_e}{n_c} k^2 \psi = 0, \quad (1)$$

where ψ is the slowly varying envelope representation of the x-ray probe, and $k = 2\pi/\lambda$ is the wave number of x-ray field in free space. Assume

$$\psi(x, z) = A(x, z) \exp[i\varphi(x, z)], \quad (2)$$

where both the amplitude $A(x, z)$ and the phase $\varphi(x, z)$ are real functions. Substituting Eq. (2) into Eq. (1) yields

$$2kA \frac{\partial \varphi}{\partial z} + A \left(\frac{\partial \varphi}{\partial x} \right)^2 - \frac{\partial^2 A}{\partial x^2} + \frac{n_e}{n_c} k^2 A = 0 \quad (3)$$

and

$$2k \frac{\partial A}{\partial z} + 2 \frac{\partial A}{\partial x} \frac{\partial \varphi}{\partial x} + A \frac{\partial^2 \varphi}{\partial x^2} = 0. \quad (4)$$

It is difficult to solve Eqs. (3) and (4) analytically, so we consider using approximation. First, we intend to obtain the magnitude relations for each terms of Eqs. (3) and (4). Then the approximate solutions for $A(x, z)$ and $\varphi(x, z)$ will be derived.

Denote the distribution width of the electron density as w_0 , and L the route range through which the x-ray light passes when measuring the electron density of the laser-produced plasma, normally $L/w_0 > 1$. Then one has $|\partial n_e / \partial x| \sim |\partial n_e / \partial z| \sim n_{e\max} w_0$, here $n_{e\max}$ denotes the maximum of the electron density of the laser-produced plasma. By making use of WKBJ solutions, one has the magnitude relations for phase, i.e., $|\partial \varphi / \partial x| \sim (kL/2w_0)(n_{e\max}/$

*Author to whom correspondence should be addressed. FAX: +86-20-8521-1603. Email address: hguo@snu.edu.cn

n_c), $|\partial^2\varphi/\partial x^2| \sim (kL/2w_0^2)(n_{e\max}/n_c)$, and $|\partial\varphi/\partial z| \sim (k/2) \times (n_{e\max}/n_c)$, respectively. The magnitude of the derivatives of the amplitude is supposed to satisfy $|\partial A/\partial x| \sim |\partial A/\partial z| \sim A/W$, where W is the characteristic length of the amplitude variation when propagating through plasma. Thus the magnitude of each terms in Eq. (3) can be obtained

$$2kA \left| \frac{\partial\varphi}{\partial z} \right| \sim Ak \frac{\eta}{\delta L}, \quad (5a)$$

$$A \left(\frac{\partial\varphi}{\partial x} \right)^2 \sim \frac{1}{4} Ak^2 \eta^2, \quad (5b)$$

$$\left| \frac{\partial^2 A}{\partial x^2} \right| \sim \frac{1}{16} Ak^2 \left(1 - \frac{\eta}{2} \right)^{-2} \delta^2 \eta^2, \quad (5c)$$

$$\frac{n_e}{n_c} k^2 A \sim Ak \frac{\eta}{\delta L}. \quad (5d)$$

Similarly, for Eq. (4), one has

$$2k \left| \frac{\partial A}{\partial z} \right| \sim \frac{1}{2} Ak^2 \left(1 - \frac{\eta}{2} \right)^{-1} \delta \eta, \quad (6a)$$

$$2 \left| \frac{\partial A}{\partial x} \frac{\partial\varphi}{\partial x} \right| \sim \frac{1}{4} Ak^2 \left(1 - \frac{\eta}{2} \right)^{-1} \delta \eta^2, \quad (6b)$$

$$A \left| \frac{\partial^2\varphi}{\partial x^2} \right| \sim \frac{1}{2} Ak^2 \delta \eta, \quad (6c)$$

where $\delta = 1/kw_0 = \lambda/2\pi w_0 \ll 1$, and it can be verified that $W = 4w_0(1 - \eta/2)/\eta$. In the above relations, we have introduced a parameter η ,

$$\eta = \frac{L}{w_0} \frac{n_{e\max}}{n_c}. \quad (7)$$

The importance of η will become more clear in the following discussions. Now we give some basic physical significance of η . From the figures in Ref. [13], we found that the error is smaller with smaller L/w_0 's and $n_{e\max}/n_c$'s. Hence the parameter η is related to the errors due to approximate solutions of φ and can be used to evaluate the errors of the electron-density measurement. Further, we will prove by numerical simulation that, η takes the role as a criterion factor to judge the validity scope of x-ray interferometric technique in measuring the electron density.

It is known that the light cannot propagate in plasma with $n_e > n_c$ [2,3] and hence cannot be used as the probe light. In the following discussions, this can be satisfied by simply letting $\eta < 1$ (since normally $L/w_0 > 1$). Since Eqs. (3) and (4) are derived from Eq. (1), we should consider the magnitudes for all terms in both equations together in analysis. The ratio for these terms is

$$(5a):(5d):(5b):(6a):(6c):(6b):(5c) \\ = 1:1:\frac{L}{w_0} \frac{\eta}{4}:\frac{1}{2} \frac{L}{w_0} \delta \left(1 - \frac{\eta}{2} \right)^{-1}:\frac{1}{2} \frac{L}{w_0} \delta:\frac{1}{4} \frac{L}{w_0} \delta \eta \left(1 - \frac{\eta}{2} \right)^{-1}:\frac{1}{16} \frac{L}{w_0} \eta \delta^2 \left(1 - \frac{\eta}{2} \right)^{-2}. \quad (8)$$

According to the above equation, when $\eta < 1$, Eq. (5c) is the smallest among all terms in Eqs. (3) and (4), so it has little effect on the change of A and φ and can be ignored in the following discussions. Since $A \neq 0$, Eq. (3) can be rewritten as

$$2k \frac{\partial\varphi}{\partial z} + \left(\frac{\partial\varphi}{\partial x} \right)^2 + \frac{n_e}{n_c} k^2 = 0, \quad (9)$$

which implies that the evolution of φ is only dependent on n_e and is decoupled from A . Therefore, Eq. (9) governs the evolution of phase of the x-ray probe in laser-produced plasma, and Eq. (4) indicates that the evolution of amplitude of x-rays is only dependent on the transverse variation of φ . It is also found from Eq. (8) that all terms of Eq. (3) except the third one are $\eta(1 - \eta/2)/(2\delta)$ greater than those of Eq. (4) by making using of Eq. (8). Hence, generally, we only consider the change of φ and ignore the change of A when η is small enough. Furthermore, it can be found that the change of amplitude is much less than that of phase after the x-rays propagate through the laser-produced plasma. In the following we will derive a series of high-order approximate solutions of φ and A for different range of η and discuss the feasibility of extending the validity scope of x-ray interferometry.

When $\eta \ll 1$, we can ignore Eq. (4) and the second term of Eq. (9). Then we obtain the solutions that coincide with the WKB solutions,

$$A^{(0)}(x, z) = A_0, \quad (10)$$

$$\varphi^{(0)}(x, z) = \varphi_0 - \frac{k}{2n_c} \int_0^z n_e(x, z') dz',$$

where A_0 and φ_0 is the initial value of the amplitude and the phase of the probe light, respectively (φ_0 is also the phase of the x-ray reference light). Here the solutions are viewed as the zeroth order approximate solutions. When η gets a little bit greater, modification should be made and the first-order approximate solution of the phase can be obtained if the second term of Eq. (9) can be used as a perturbation. Substituting the zeroth order solution of phase, i.e., Eq. (10), into Eq. (9) yields

$$\varphi^{(1)}(x, z) = \varphi_0 - \frac{k}{2n_c} \int_0^z dz' n_e(x, z') - \frac{1}{2k} \int_0^z dz' \\ \times \left[\frac{\partial\varphi_0(x, z')}{\partial x} - \frac{k}{2n_c} \int_0^{z'} \frac{\partial n_e(x, z'')}{\partial x} dz'' \right]^2. \quad (11)$$

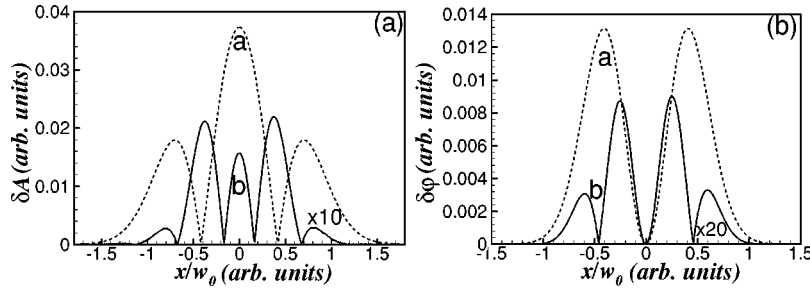


FIG. 1. Comparison of the relative errors of amplitude and phase between the exact and the approximate solutions when n_e is the Gaussian profile and $A = 100.0, L/w_0 = 5$, in which (a) and (b) denote the errors of the amplitude and the phase, respectively. In (a), curves a (dashed line) and b (solid line) denote the dependence of $\delta A^{(0)}$ and $\delta A^{(1)} (\times 10)$, respectively, versus the normalized transverse coordinate x/w_0 . In (b), curves a (dashed line) and b (solid line) denote the dependence of $\delta\varphi^{(0)}$ and $\delta\varphi^{(1)} (\times 20)$, respectively, versus the normalized transverse coordinate x/w_0 . Here, $\eta = 0.05$, $\delta A_{\max}^{(0)} \approx 3.7\%$, $\delta A_{\max}^{(1)} \approx 0.2\%$, $\delta\varphi_{\max}^{(0)} \approx 1.3\%$, and $\delta\varphi_{\max}^{(1)} \approx 0.045\%$.

It is evident that the above solution coincides with the modified solution given in Ref. [13] if $\varphi_0 = \text{const}$. In this condition the amplitude may also be modified. When η gets much greater and is close to unity (but $\eta < 1$ is still valid), higher-order solutions, $\varphi^{(n)}$ ($n > 1$), should be derived by substituting lower-order solutions, $\varphi^{(n-1)}$ ($n > 1$), into Eq. (9) iteratively to approach the exact value. Meanwhile, Eq. (4) should be taken into account since the change of amplitude is sufficiently efficient and has affected the measurement. Analogous to the higher-order solutions of phase, the higher-order solutions of amplitude can also be derived by using iterative substituting method since the orders of the second and the third terms of Eq. (4) are much less than that of the first term, and so both terms can be used as perturbations. Then the higher-order solutions of phase and amplitude yield

$$\varphi^{(n)}(x, z) = \varphi^{(0)} - \frac{1}{2k} \int_0^z \left[\frac{\partial \varphi^{(n-1)}(x, z')}{\partial x} \right]^2 dz' \quad (12)$$

and

$$A^{(n)} = A_0 \exp \left[-\frac{1}{k} \int_0^z \frac{\partial A^{(n-1)}(x, z')}{\partial x} \frac{\partial \varphi^{(n-1)}(x, z')}{\partial x} dz' \right] \times \exp \left[-\frac{1}{2k} \int_0^z \frac{\partial^2 \varphi^{(n-1)}(x, z')}{\partial x^2} dz' \right], \quad (13)$$

respectively. It is evident that so long as $\eta < 1$, then $\lim_{n \rightarrow \infty} \eta^n = 0$, and the powers of η can be used to derive the magnitude relations shown in Eqs. (8). Therefore, at least in principle, so long as $\eta < 1$, a more precise relation for electron-density measurement is achievable, provided that the order of the iterative substituting solutions, n , shown in Eqs. (12) and (13) can be as large as one wants ($n \rightarrow \infty$) and the solutions can approach the exact solutions, where the effects of higher-order gradients of the electron density, i.e., $(\partial n_e / \partial x)^n$ ($n \geq 1$), have been taken into account.

A numerical simulation will be made to give the higher-order solutions of $\varphi^{(n)}$ and $A^{(n)}$, while the effects of the parameter η will be demonstrated and verified. Also, the numerical solutions of Eq. (1), φ_s and A_s , will be given by making use of the split-step Fourier method [14] and will be applied as exact solutions for further analysis. Next one defines several variables to denote the relative errors for phase and amplitude, i.e., $\delta\varphi^{(i)} = |\varphi_s - \varphi^{(i)}| / |\varphi_s|_{\max}$, $\delta A^{(i)} = |A_s - A^{(i)}| / |A_0|$, where (i) is the order of the approximative solutions, s stands for the direct simulation result from Eq. (1). For the sake of simplicity, it is chosen in simulation such that $N = n_c / n_{e\max}$, $A_0 = 1$, and $\varphi_0 = 0$. Assume the electron density of the laser-produced plasma takes the Gaussian profile, i.e., $n_e(x, z) = n_c \exp(-r^2/w_0^2)/N$, where $r^2 = x^2 + z^2$ and let $\lambda = 15.5$ nm (experimentally the soft-x-ray wavelength range is 35–350 Å).

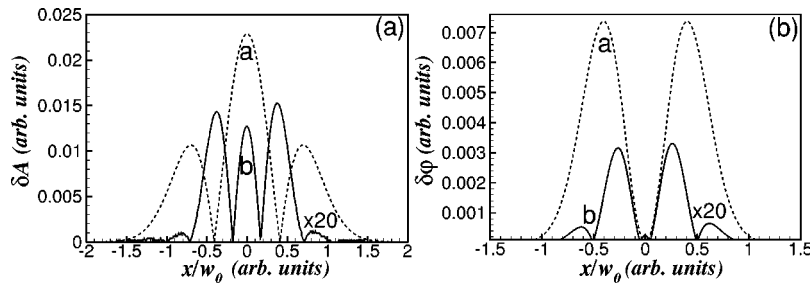


FIG. 2. Comparison of the relative errors of amplitude and phase between the exact and the approximate solutions when n_e is the Gaussian profile and $N = 100.0, L/w_0 = 3$, in which (a) and (b) denote the errors of the amplitude and the phase, respectively. In (a), curves a (dashed line) and b (solid line) denote the dependence of $\delta A^{(0)}$ and $\delta A^{(1)} (\times 20)$, respectively, versus the normalized transverse coordinate x/w_0 . In (b), curves a (dashed line) and b (solid line) denote the dependence of $\delta\varphi^{(0)}$ and $\delta\varphi^{(1)} (\times 20)$, respectively, versus the normalized transverse coordinate x/w_0 . Here, $\eta = 0.03$, $\delta A_{\max}^{(0)} \approx 2.3\%$, $\delta A_{\max}^{(1)} \approx 0.075\%$, $\delta\varphi_{\max}^{(0)} \approx 0.74\%$, and $\delta\varphi_{\max}^{(1)} = 0.015\%$.

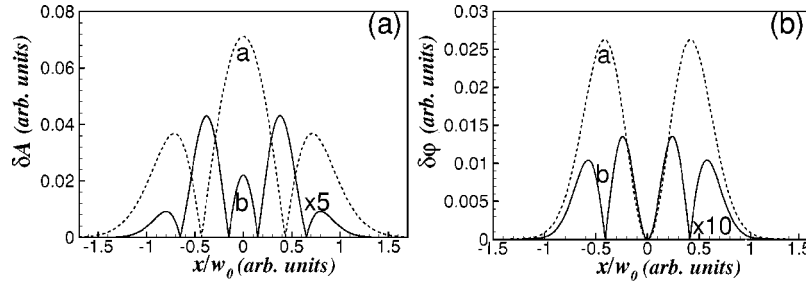


FIG. 3. Comparison of the relative errors of amplitude and phase between the exact and the approximate solutions when n_e is the Gaussian profile and $N=50.0$, $L/w_0=5$, in which (a) and (b) denote the errors of the amplitude and the phase, respectively. In (a), curves a (dashed line) and b (solid line) denote the dependence of $\delta A^{(0)}$ and $\delta A^{(1)} (\times 5)$, respectively, versus the normalized transverse coordinate x/w_0 . In (b), curves a (dashed line) and b (solid line) denote the dependence of $\delta\varphi^{(0)}$ and $\delta\varphi^{(1)} (\times 10)$, respectively, versus the normalized transverse coordinate x/w_0 . Here, $\eta=0.1$, $\delta A_{\max}^{(0)} \approx 7.1\%$, $\delta A_{\max}^{(1)} \approx 0.86\%$, $\delta\varphi_{\max}^{(0)} \approx 2.6\%$, and $\delta\varphi_{\max}^{(1)} = 0.13\%$.

The comparison of the relative errors of amplitude and phase between the exact and the approximative solutions when n_e is the Gaussian profile with different N or L/w_0 are shown in Figs. 1, 2, and 3, in which (a) and (b) denote the change of the relative errors of amplitude and phase, respectively. It can be found that (i) $\delta A^{(0)} > \delta A^{(1)}$, and $\delta\varphi^{(0)} > \delta\varphi^{(1)}$, i.e., higher-order solutions of amplitude and phase are more close to the exact solution; (ii) at the same time, the errors due to lower-order solutions are replenished by higher-order solutions for both amplitude and phase change when x-rays propagate through laser-produced plasma. The change of the amplitude is much less than that of the phase at the same conditions during numerical simulation, e.g., the maximum change of the amplitude is about 0.037 than the initial value, but for phase that is about 2026.8 when $N=100, L/w_0=5$. It is one of the main reasons that the x-ray interferometry technique can be used to measure the electron density.

Comparing Fig. 1 with Fig. 2, one finds that the relative errors for amplitude and phase become smaller with smaller L/w_0 for the same order approximation solutions where N is fixed and L/w_0 is varying. Similarly comparing Fig. 1 with Fig. 3, the errors become smaller with smaller N for the same order where L/w_0 is fixed. Comparing $\eta=(L/w_0)/N$ in three figures, one finds that for the same order solutions, greater η 's give more errors. Further, it can be found that the ratios $\delta A_{\max}^{(0)}/\delta A_{\max}^{(1)}$ and $\delta\varphi_{\max}^{(0)}/\delta\varphi_{\max}^{(1)}$ become greater with smaller

η . In other words, when η is greater, higher-order modifications are needed.

In summary, the evolution equation of phase is given, which is independent of the change of the amplitude. Also, the coupling relation between phase and amplitude is derived where the influence of amplitude on phase has been taken into account. Then a series of modified solutions for phase and amplitude can be derived. Numerically, the higher-order solutions can be derived using an iterative algorithm and it approaches the exact solutions rapidly. We found an important parameter η from magnitude analysis, which can be used to evaluate the measurement errors. At the same time, η , together with $\delta=(kw_0)^{-1}$, can be applied to analyze the magnitude relations among the terms of the propagating equation of x-ray probe. Moreover, it is justified that so long as $\eta < 1$, the modified solutions with higher-order corrections apply, and further, the x-ray interferometry is valid in measuring the electron density of plasma.

This work was partially supported by the Key Project of the National Natural Science Foundation of China (Grant No. 69789801), the Team Project of the Natural Science Foundation of Guangdong Province (Grant No. 20003061), the Foundation of National Hi-Tech Inertial Confinement Fusion Committee, the Fok Yin Tung High Education Foundation (No. 71058) and the Foundation for the Key Young Teachers of the Ministry of Education of China. Dr. H. Pu is also acknowledged for his careful reading of and some suggestions on the revised manuscript.

[1] E.F. Gabl *et al.*, Phys. Fluids B **2**, 2437 (1990).
 [2] I. H. Hutchinson, *Principles of Plasma Diagnostics with Microwave* (Cambridge University Press, Cambridge, England, 1987).
 [3] See, e.g., W. L. Kruer, *The Physics of Laser-Plasma Interactions* (Addison-Wesley, Reading, MA, 1988).
 [4] H. Soltwisch, in *Nuclear Fusion and Plasma Physics*, edited by Y. P. Huo, C. S. Liu, and F. Wagner (World Scientific, Singapore, 1995).
 [5] L.B. Da Silva *et al.*, Phys. Rev. Lett. **74**, 3991 (1995).

[6] R. Cauble *et al.*, Phys. Rev. Lett. **74**, 3816 (1995).
 [7] C.H. Moreno *et al.*, Phys. Rev. E **60**, 911 (1999).
 [8] A.S. Wan *et al.*, J. Opt. Soc. Am. B **13**, 447 (1996).
 [9] A.S. Wan *et al.*, Phys. Rev. E **55**, 6293 (1997).
 [10] C. Darrow *et al.*, J. Appl. Phys. **67**, 3630 (1990).
 [11] D. Ress *et al.*, Science **265**, 514 (1994).
 [12] R. A. London, Phys. Fluids **31**, 184 (1988).
 [13] Hong Guo *et al.*, Phys. Rev. E **63**, 066401 (2001).
 [14] Govind P. Agrawal, *Nonlinear Fiber Optics*, 2nd ed. (Academic Press, San Diego, 1995).